COMPOSITE: JOURNAL OF CIVIL ENGINEERING
UNIVERSITAS MERDEKA MALANG

ISSN-P: 2964-6626 ISSN-E: 2961-7111

▪ Construction Engineering ▪ Transportation Engineering ▪ Water Engineering ▪ Environmental Engineering ▪ Construction Management ▪ Geotechnical Engineering ▪ Occupational Health and Safety in Construction ▪ Construction and Environment Law.

COMPOSITE: JOURNAL OF CIVIL ENGINEERING
2025. Vol. 04. Number. 02: 44-54

Available (PDF): https://jurnal.unmer.ac.id/index.php/jtsc

The Effect of CFRP Flexural Reinforcement on Ductility, Stiffness, and Energy Dissipation of T-Beam Numerically

Andhika Mahendra[1], Muslikh[2]

[1]Universitas Tanri Abeng, Jakarta Selatan 12250, Indonesia
[2]Universitas Gadjah Mada, Yogyakarta 55281, Indonesia

Keywords:
CFRP; Ductility; Energy Dissipation; Numerical; Stiffness

Abstract
Structural damage in Indonesia often occurs due to disasters and lack of maintenance. Structural strengthening is needed to keep buildings functioning, one of which is with CFRP (Carbon Fiber Reinforced Polymer) which is known to be able to increase load capacity. However, CFRP can reduce ductility, making the structure stiffer and brittle, which is at risk of structural failure. This study examines the effect of CFRP flexural strengthening on post-crack T-beams using the finite element method validated with previous experimental data. Three variations were tested: a control beam, a beam with CFRP along the span, and a half-span CFRP. The results show that the stiffness of the simulation is higher than the experiment due to ideal conditions in the numerical, whereas, the experimental study occurred unjustified slip. The difference in yield load and maximum load is less than 5%, indicating a valid simulation. Test results with various CFRP lengths show that the fully reinforced beam shows the best performance with increased load capacity and energy dissipation.

Kata Kunci:
CFRP; Daktilitas; Disipasi Energi; Kekakuan; Numerik

Abstrak
Kerusakan struktur di Indonesia sering terjadi akibat bencana dan kurangnya perawatan. Perkuatan struktur diperlukan agar bangunan tetap berfungsi, salah satunya dengan CFRP (Carbon Fiber Reinforced Polymer) yang dikenal mampu meningkatkan kapasitas beban. Namun, CFRP dapat menurunkan daktilitas, membuat struktur menjadi lebih kaku dan getas, yang berisiko kegagalan struktur. Penelitian ini mengkaji pengaruh penguatan lentur CFRP pada balok T pasca retak menggunakan metode elemen hingga yang divalidasi dengan data eksperimen sebelumnya. Tiga variasi diuji: balok kontrol, balok dengan CFRP sepanjang bentang, dan CFRP setengah bentang. Hasil menunjukkan bahwa kekakuan dari simulasi lebih tinggi dari eksperimen dikarenakan keadaan ideal pada numerik sedangkan, studi eksperimental terjadi slip yang tidak bisa dijustifikasi. Perbedaan beban leleh dan beban maksimum kurang dari 5%, menunjukkan simulasi valid. Hasil pengujian dengan variasi panajang CFRP menunjukkan balok dengan penguatan penuh menunjukkan kinerja terbaik dengan peningkatan kapasitas beban dan disipasi energi.

Article History:
Submitted: 15 Oktober 2025
Accepted: 29 November 2025
Available Online: 31 Desember 2025

Korespondensi Penulis:
Andhika Mahendra

Email:
andhika@tau.ac.id

Sitasi: *Mahendra, A., & Muslikh, M. The Effect of CFRP Flexural Reinforcement on Ductility, Stiffness, and Energy Dissipation of T-Beam Numerically. Composite: Journal of Civil Engineering, 4(2). https://doi.org/10.26905/cjce.v4i2.16302*

1. Introduction

Many building structures in Indonesia have been damaged by natural disasters and poor structural maintenance. In addition, many building structures in Indonesia use the standards of the old building regulations but, if the structure is compared with the latest regulations, the structure becomes unsafe. Strengthening the building structure is the best way so that the building can be used as planned. One of the well-known and easy-to-apply reinforcement is CFRP (Carbon Fiber Reinforced Polymer). However,

the reinforced structure not only has a positive impact due to the increase in load capacity but, it also has a negative impact on the structure. The negative impact is an increase in the stiffness of the structure which means its ductility decreases. This is very dangerous for the structure because the structure can collapse suddenly if it has exceeded its load capacity. Therefore, the effect of flexural reinforcement on ductility, stiffness, and energy dissipation of T-beams needs to do so that the applied reinforcement does not cause sudden collapse. Experimental testing needs to do, however, numerical simulation is also necessary because experimentally validated numerical simulations can be a tool to carry out advanced parameter studies and this can save costs without the need to make test objects again.

This research simulates the experimental research conducted by (Mulyanto, 2020), where it conducted a study that aims to determine the behavior of CFRP-reinforced T-beams in the flexural section. Tests were carried out using four-point bending. The variables analyzed were ductility, flexural stiffness, flexural load capacity, crack, and failure patterns. The effect of adding CFRP can also be seen in previous studies. Recent research has extensively validated the efficacy of Fiber-Reinforced Polymer (FRP) composites in enhancing reinforced concrete (RC) elements, particularly in addressing complex structural deficiencies and challenging environmental conditions. Studies have confirmed CFRP's capability to restore integrity to compromised members, such as RC beams with web openings subjected to cyclic loading, where strengthening was shown to recover lost capacity and increase maximum strength by up to 66.67% (Salih et al., 2020). This restorative capacity extends to members degraded by material deterioration; for example, CFRP strengthening was found to increase the peak load of beams with corroded internal steel by up to 90% while substantially restoring their energy dissipation capacity (Kim et al., 2025). Similarly, in seismic contexts, CFRP wrapping has been shown to be effective for retrofitting recycled concrete columns with pre-existing seismic damage, with the strengthening effect being most significant for columns with low to medium initial damage (displacement ratio less than 3%) (Song et al., 2023). Beyond pure restoration, a critical focus has been the mitigation of premature debonding. To this end, innovative anchorage systems have been developed, such as a groove-epoxy system for shear strengthening, which successfully delayed failure and enhanced shear capacity by up to 141% (Mohamed et al., 2024). In parallel for flexural strengthening, spike anchors have been employed effectively to prevent debonding, increasing average load capacity by 19% over unanchored beams and enabling better utilization of the CFRP's strength (Assad et al., 2024).The specific performance of FRP is also highly dependent on material interactions. For instance, it has been observed that while CFRP wrapping is effective for both normal-weight (NWC) and lightweight concrete (LWC), the enhancement in compressive strength, ductility, and failure mode was significantly more pronounced for LWC (Hawileh et al., 2024). This comparative approach has also led to innovations in the fiber materials themselves. Studies comparing conventional Carbon (CF) and Glass (GF) fibers against ductile Polyethylene Terephthalate (PET) fibers for seismic retrofitting concluded that PET fibers provide comparable strength enhancement while exhibiting vastly superior ductility and a safer, non-brittle failure mode (Choi et al., 2021).From previous research, This study differs in that the tested T-beam is in a post-crack state, numerically simulated using the finite element method. This type of post-crack T-beam modeling has never been done before. Based on previous research it can be seen that the addition of CFRP can increase the load capacity and some add to the ductility of the test object. Therefore, this research was very important to do. This study aims to determine the effect of CFRP length on ductility, stiffness, and energy dissipation in T-beams in post-crack condition.

2. Methods

This study performed a numerical simulation using the finite element method of T-beam reinforced with CFRP. The T-beam modeling followed the experimental tests that have been carried out by (Mulyanto, 2020). The loading given was four-point bending where the loading consists of loads up to the first crack then, repeated loads, and finally loads until the T-beam collapsed. The modeling consisted of three models, namely control beams, reinforced beams along the span, and half-span reinforced beams. The most optimum reinforcement to be applied was assessed in terms of strength, ductility, stiffness, and energy dissipation.

According to (Park & Paulay, 1975) ductility was the ability of a structure to experience a large enough deflection when the maximum load reached before it collapsed. According to (Tawil & G. G. Deierlein, 1999) the ductility curve of the cross-section ($\mu\phi$) defined as shown **Figure 1**.

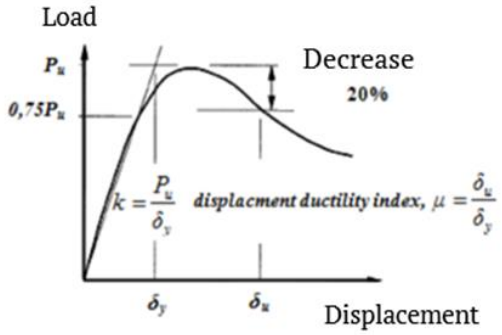

Figure 1. Definition of Ductility Ratio Curve

Source : (Tawil & G. G. Deierlein, 1999)

According to Gere & Stephen P. Timoshenko, 1996, that stiffness was defined as the force required to produce a deflection of one unit, the stiffness value was the slope of the line from the relationship between load and deflection. According to J. J. Sudjati, 2007, energy dissipation was the ability of a structure to absorb energy through the melting process in the plastic hinge area. The capacity of the energy could be calculated from the area under the load-deflection curve using the trapezoidal method.

Material Properties

The numerical simulation required the idealization of the material used in the modeling. In this case, the materials used were concrete, reinforcing steel, epoxy, and CFRP. These materials were used to approximate the experimental results that had been carried out previously.

Parameters of concrete material were compressive and tensile behavior which were approximated by the (Mander et al., 1989) equation for compressive strength and fracture energy for tensile strength. This behavior could be seen in **Figure 2** and **Figure 3**. The rebar steel material in the form of a stress-strain relationship was close to the (Park & Paulay, 1975) model. The graphic image of the stress-strain relationship of steel could be seen in **Figure 4**.

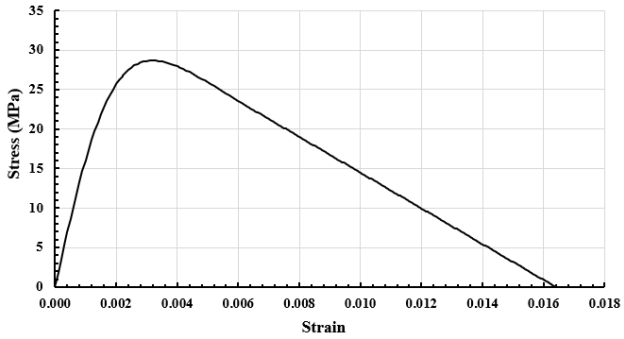

Figure 2. Concrete Compressive Stress-Strain Model

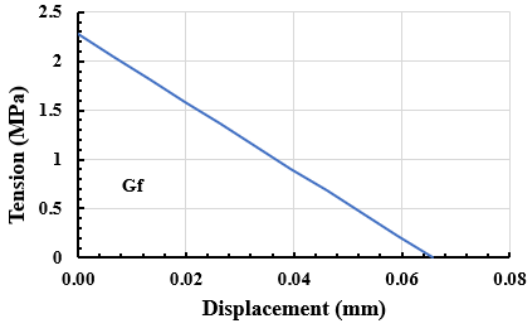

Figure 3. Concrete Tensile Stress-Displacement Model of ABAQUS Manual

Source : (Abaqus, 2016)

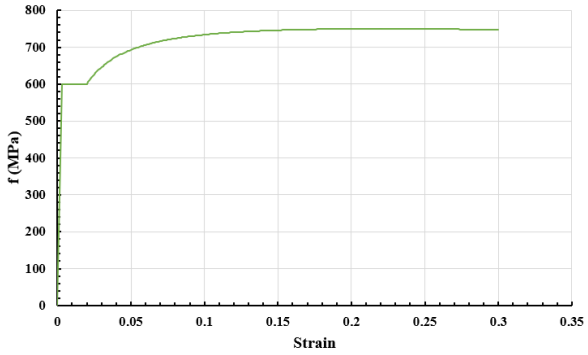

Figure 4. Bar Steel Stress-Strain Model

CFRP was one of the well-known reinforcements to apply because it is light, non-corrosive, and has high strength. The characteristics of the SikaWrap 231C CFRP material included the modulus of elasticity, shear modulus, and others as listed in **Table 1**. Meanwhile, the adhesive or glue for bonding CFRP with concrete used Sikadur-330 Epoxy. The modeling of the adhesive material was idealized as a cohesive zone interaction (Kabir et al., 2016), which was approximated according to equations 1 and 2. The material parameters of the epoxy are shown in **Table 2**.

Table 1. Parameter properties of CFRP

Exp.	Value	Exp	Value
E1	221.500 MPa	G12	13.540 MPa
E2	21.670 MPa	G13	13.540 MPa
E3	21.670 MPa	G23	11.790 MPa
$\boldsymbol{\nu_{12}}$	0,31	XT	3.000 MPa
$\boldsymbol{\nu_{13}}$	0,31	XC	2.200 MPa
$\boldsymbol{\nu_{23}}$	0,31	SL	97 MPa
$\boldsymbol{G_{ft}^{c}}$	45 mJ	$\boldsymbol{G_{fc}^{c}}$	0,6 mJ
$\boldsymbol{G_{mt}^{c}}$	45 mJ	$\boldsymbol{G_{mc}^{c}}$	0,6 mJ
YT	82 MPa	$\boldsymbol{\eta_{fc}}$	0,003
YC	236 MPa	$\boldsymbol{\eta_{mt}}$	0,003
ST	97 MPa	$\boldsymbol{\eta_{mc}}$	0,003
$\boldsymbol{\eta_{ft}}$	0,003		

Table 2. Parameter Properties of Epoxy

Parameter	Explanation
Density	1,30 kg/liter
Elasticity Modulus	4.563 MPa
Shear Modulus	1.665,3285 MPa
Elongation at break	0,9%
Adhesion compressive strength	> 2 MPa

$$K_{nn} = \frac{E_a}{T_0} \quad (1)$$

$$K_{ss} = K_{tt} = 3\left(\frac{G_a}{T_0}\right)^{0.65} \quad (2)$$

Test Object Model

The test object model in this study was a test object made by (Mulyanto, 2020). This modeling used the help of the ABAQUS software, and all dimensions followed the experimental research. **Figure 5** showed the geometric data of the specimen to be modeled in ABAQUS, and the full model could be seen in **Figure 6**. The elements in the numerical simulation must be idealized according to their needs. These elements were:

1. Concrete beams and solid steel loads and supports were modeled with 3D solid elements in the form of C3D8R elements (3D continuum, 8–node linear brick, reduced integration).

2. The reinforcing steel modeled with T3D2 truss elements (3D truss, 2–node linear truss)
3. CFRP was modeled with a three-dimensional conventional shell element in the form of an S4R element (shell, 4-node, reduced integration with hourglass control, finite membrane strains).

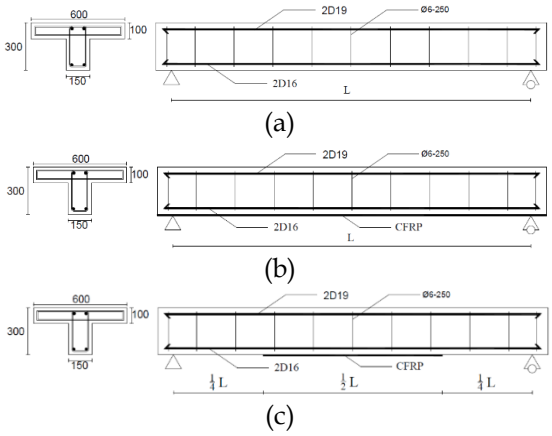

Figure 5. T-beam Specimens: (a) Control Beam, (b) T-beam with Reinforcement along The Span (B1), (c) T-beam with Reinforcement Half of The Span (B2)

Source : (Mulyanto, 2020)

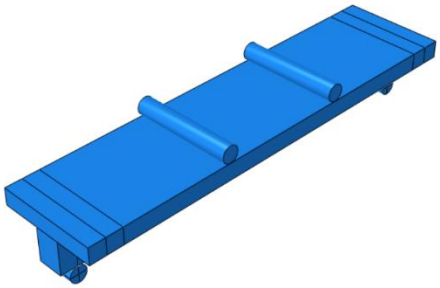

Figure 6. Full Model Numerical Simulation of T-Beam

3. Result and Discussion

Load – displacement curve

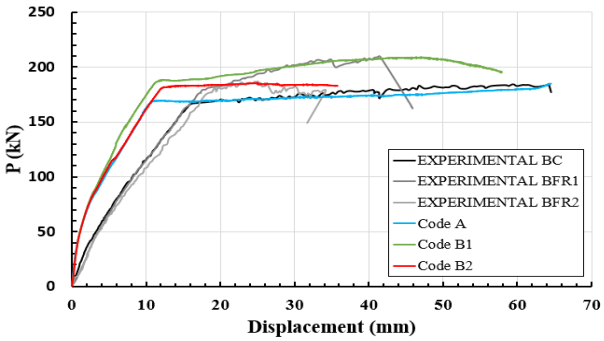

Figure 7. Load-Displacement Curve

Table 3. The Comparison Ultimate Load between Experimental and Numeric

Explanation	Pu (kN)	The Difference Pu (%)
Experimental BC	184.800	–
A	184.842	0.0227
Experimental BFR1	209.700	–
B1	208.387	–0.6261
Experimental BFR2	186.700	–
B2	185.191	–0.8082

From the load-displacement curve as shown in **Figure 7,** the numerical simulations were well-validated than experimental because the curve between them is similar. The value of the ultimate load between experimental and numerical can be seen in **Table 3**. From it, we can conclude that the difference or error between experimental and numeric was less than 5%. So, the simulation of this research had a good agreement.

Ductility

The results of ductility were presented in Figures 8, 9, and 10, and comparisons with experimental results are summarized in Table 4.

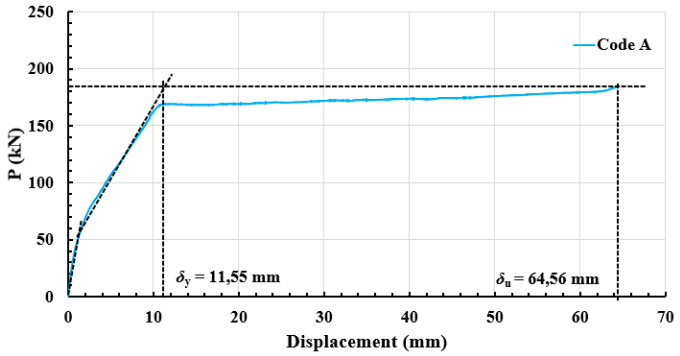

Figure 8. The Ductility of Code A

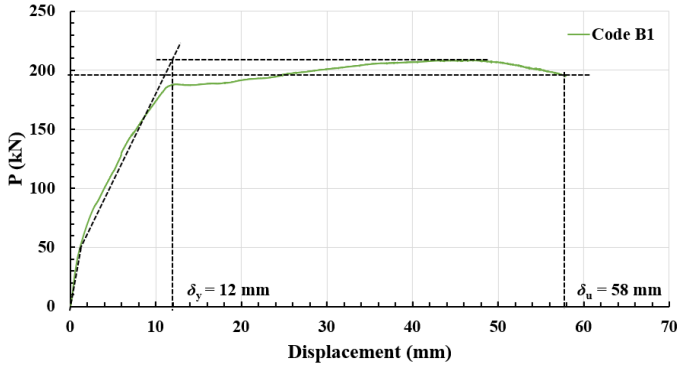

Figure 9. The ductility of code B1

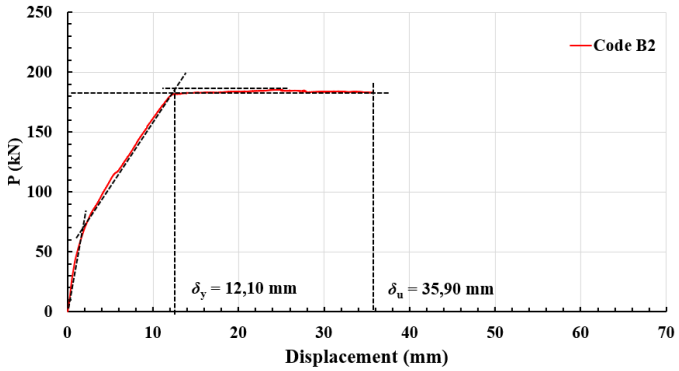

Figure 10. The Ductility of Code B2

Table 4. The Ductility Value of Specimens

Test Object Code	δ_y (mm)	δ_u (mm)	Ductility $\mu = \delta_u / \delta_y$	Decreasing (%)	Experimental Ductility	Experimental Decreasing (%)
A	11.55	64.56	5.5896	–	3.58	–
B1	12.00	58.00	4.8333	13.5300	2.31	35.54
B2	12.10	35.90	2.9669	46.9204	1.70	52.69

The ductility behavior in numerical simulations with experimental ones was similar. This behavior was a decrease in ductility with the addition of CFRP when compared to unreinforced beams. Determination of stopping running and displacement was when the model was no longer convergent, even though the model could still perform iterations; however, the increment that occurs was very small and would take a very long time. Therefore, when the model experiences very small convergence like this, the model will automatically stop running, and this also depends on how small the incremental step was requested or set in ABAQUS.

In determining the ductility value, it is necessary to determine the deflection value at yield (δ_y) and the maximum deflection (δ_u). **Figures 8 – 10** show the graph of the relationship between load and deflection for each variation and the determination of the δ_y and δ_u values. Then, these values are calculated to obtain the ductility value for each variation. From **Table 4**, the ductility behavior in the experimental and numerical simulations has the same trend, namely, with the addition of CFRP, the ductility value of the T-beam decreases. And as the length of the CFRP decreases, the ductility value also decreases. In this study, the length of the CFRP, which was initially along the span, experienced a smaller decrease compared to the half-span length of the T-beam.

Stiffness

The results of stiffness were presented in **Figures 11, 12, and 13** and comparisons with experimental results were summarized in **Table 5, 6, 7, and 8**.

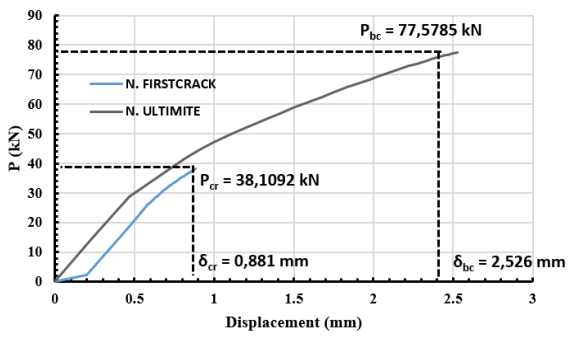

(a)

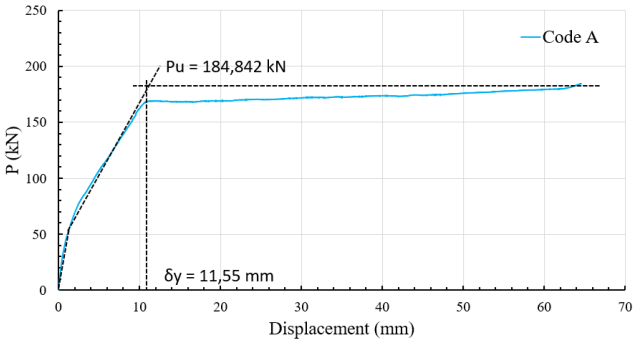

(b)

Figure 11. The Stiffness of Code A

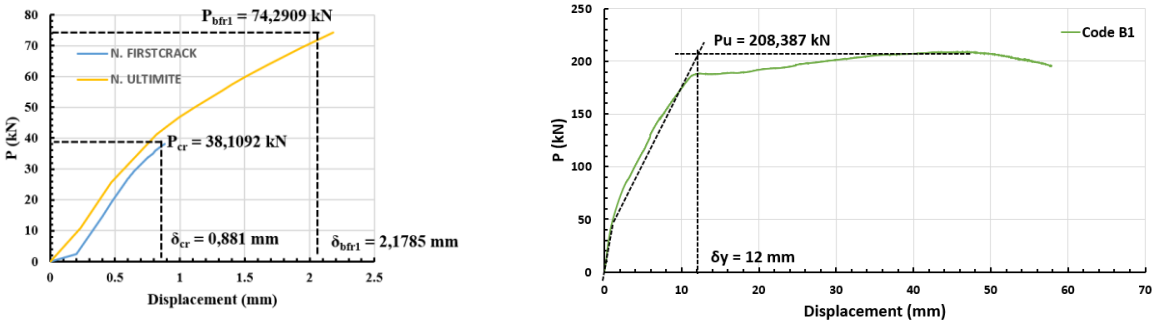

(a) (b)

Figure 12. The Stiffness of Code B1

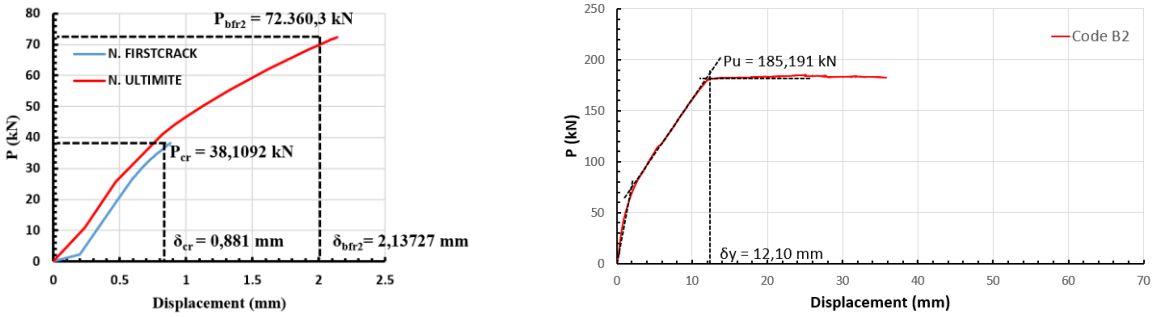

(a) (b)

Figure 13. The Stiffness of Code B2

Table 5.

Table 5. The Stiffness Result before Repeated Loading

Test Object Code	P_{cr} (N)	δ_{cr} (mm)	Stiffness (N/mm)	Ratio	Experimental Stiffness (N/mm)	Ratio
A	38,109.2	0.881	43,256.75	–	11,048.03	–
B1	38,109.2	0.881	43,256.75	–	13,214.29	1.20
B2	38,109.2	0.881	43,256.75	–	10,746.89	1.23

Table 6. The Stiffness Result after Repeated Loading

Test Object Code	P_{cr} (N)	δ_{cr} (mm)	Stiffness (N/mm)	Ratio	Experimental Stiffness (N/mm)	Ratio
A	77,578.5	2.52600	30,712.00	–	10,541.67	–
B1	74,290.9	2.17850	34,101.86	1.1104	13,489.58	1.28
B2	72,360.3	2.13727	33,856.41	1.1024	12,950.00	1.23

Table 7. The Stiffness Result "Before" and "After" Repeated Loading

Test Object Code	The stiffness before repeated load (N/mm)	The stiffness after repeated load (N/mm)	Ratio (after/before)
A	43,256.75	30,712.00	0.7100
B1	43,256.75	34,101.86	0.7884
B2	43,256.75	33,856.41	0.7827

Table 8. The Equivalent Stiffness Results in Each Model

Test Object Code	$P_y = P_u$ (N)	δ_y (mm)	Stiffness (N/mm)	Ratio	Experimental Stiffness (N/mm)	Ratio
A	184,842	11.55	16,003.64	–	10,021.74	–
B1	208,387	12	17,365.58	1.085	10,644.67	1.062
B2	185,191	12.10	15,305.04	0.956	9,983.96	0.996

From the flexural stiffness results obtained, the numerical and experimental results had quite a large difference. This could also be seen from the comparison of the load-deflection curves, which also had quite a large difference. This is because unjustified slippage often occurs in experimental testing, whereas numerical simulations are idealized and free of noise. Because of this, experimental tests experienced energy loss in their lab tests due to slippage. This led to significant differences in test results and higher numerical results compared to the experimental results. However, the above results showed similar behavior between the numerical results and the experimental results.

Figures 11-13 show the stiffness values of each test specimen variation. Point A is the initial stiffness value, and point B is the equivalent stiffness value. **Tables 5-8** are the stiffness values of the test specimens before and after repeated loading and the equivalent stiffness values. Beam B1 has the greatest stiffness value compared to the experimental T-beam and beam B2. However, beam B2 has a smaller stiffness value compared to the experimental T-beam and beam B1. Thus, the addition of CFRP is able to increase the stiffness of the T-beam and occurs only when the CFRP is added along the span. Meanwhile, beam B2 with the addition of half the span length is almost similar to the stiffness value of the T-beam without the addition of CFRP.

3.1 Dissipation Energy

The results of energy dissipation were presented in **Figures 14** and comparisons with experimental results were summarized in **Table 9 and 10**.

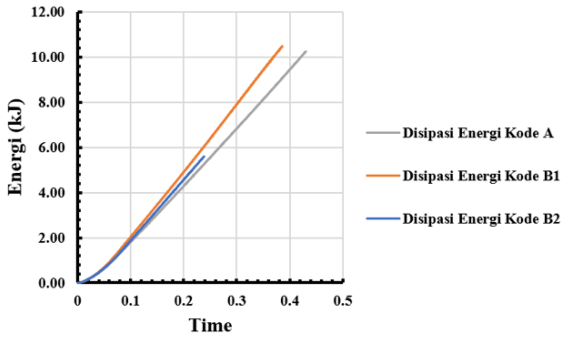

Figure 14. Energy-time curve

Table 9. The comparison of energy dissipation results by two methods

Test Object Code	The Trapezoidal Method (kJ)	*Output* ABAQUS (kJ)	The Difference (%)
A	10.493	10.243	2.3822
B1	10.656	10.478	1.6723
B2	5.740	5.595	2.5232

Table 10. The comparison of the behavior of ABAQUS and experimental energy dissipation results

Test Object Code	*Output* ABAQUS (kJ)	Ratio	Experimental (kJ)	Ratio
A	10,243	–	6.860	–
B1	10,478	1.023	7.391	1.077
B2	5,595	0.546	5.057	0.737

Figure 14 shows the energy dissipation rate versus time generated by the numerical simulation. **Table 10** compares the energy dissipation results from the experimental and numerical tests. The results of energy dissipation showed that the calculation using the area graph method and the output from ABAQUS had similar values. This was because the difference in energy values was less than 5%. The increase in energy only occurred in the code B1 beam, where the CFRP applied was along the beam. From the energy results in experimental testing, the behavior of the results was the same as the numerical results. Where CFRP flexural strengthening to increase energy capacity could only be done by applying it to the entire beam span.

4. Simpulan

The results of the numerical modeling are well validated, where the ultimate load value obtained from the numerical modeling has a difference of less than 5%. The addition of CFRP to the ductility of the T-beam can reduce the ductility value, especially in the test specimen with the addition of CFRP half-span. Then, the stiffness increases due to the addition of CFRP. Beam B1 has the greatest energy dissipation compared to other test specimen variations. From these results, it can be concluded that the addition of CFRP with variations along the span (B1) has the best and most optimum value. Therefore, repairing building structures that have cracked is recommended to use CFRP reinforcement with a full length or along the span.

5. Daftar Pustaka

Abaqus, S. (2016). *Abaqus Analysis User's Guide*. http://130.149.89.49:2080/v2016/books/usb/default.htm

Assad, M., Hawileh, R. A., & Abdalla, J. A. (2024). Flexural Strengthening of Reinforced Concrete Beams with CFRP Laminates and Spike Anchors. *Composites Part C: Open Access*, *13*(February), 100443. https://doi.org/10.1016/j.jcomc.2024.100443

Choi, D., Hong, S., Lim, M. K., Ha, S. S., & Vachirapanyakun, S. (2021). Seismic Retrofitting of RC Circular Columns Using Carbon Fiber, Glass Fiber, or Ductile PET Fiber. *International Journal of Concrete Structures and Materials*, *15*(1). https://doi.org/10.1186/s40069-021-00484-7

Gere, J. M., & Stephen P. Timoshenko. (1996). *Mekanika Bahan*. Erlangga Jakarta.

Hawileh, R. A., Alharmoodi, H., Hajjaj, A., Aljarwan, A., & Abdalla, J. A. (2024). Effect of CFRP Wraps on the Compressive Strength of Normal and Structural Lightweight Concrete. *Procedia Structural Integrity*, *54*, 279–286. https://doi.org/10.1016/j.prostr.2024.01.084

J. J. Sudjati. (2007). *Peningkatan Disipasi Energi dan Daktilitas pada Kolom Beton Bertulang yang Diretrofit dengan Carbon Fiber Jacket*.

Kabir, M. H., Fawzia, S., Chan, T. H. T., & Badawi, M. (2016). Numerical Studies on CFRP Strengthened Steel Circular Members Under Marine Environment. *Materials and Structures/Materiaux et Constructions*, *49*(10). https://doi.org/10.1617/s11527-015-0781-5

Kim, S., Choi, W., & Kim, J. (2025). Performance Evaluation of Reinforced Concrete Beams with Corroded Rebar Strengthened by Carbon Fiber-Reinforced Polymer. *Polymers*, *17*(8). https://doi.org/10.3390/polym17081021

Mander, J. B., Priestley, M. J. N., & Park, R. (1989). The Oretical Stress-Strain Model for Confined Concrete. *J. Struct. Eng*, *114*(8), 1804–1826.

Mohamed, K., Abdalla, J. A., Hawileh, R. A., & Musa, A. E. S. (2024). Experimental and Analytical Investigations of the Use of Groove-Epoxy Anchorage System for Shear Strengthening of RC Beams Using CFRP Laminates. *Structures*, *70*. https://doi.org/10.1016/j.istruc.2024.107676

Mulyanto, T. (2020). *Perilaku Pengaruh Penambahan Perkuatan CFRP terhadap Kekuatan Lentur Balok–T*. Universitas Gadjah Mada.

Park, R., & Paulay, T. (1975). *Reinforced Concrete Structures*. A Wiley Interscience Publication.

Salih, R., Zhou, F., Abbas, N., & Mastoi, A. K. (2020). Experimental Investigation of Reinforced Concrete Beam with Openings Strengthened using FRP Sheets Under Cyclic Load. *Materials*, *13*(14). https://doi.org/10.3390/ma13143127

Song, S., Tian, Z., Zhao, Z., Li, X., Zhao, J., & Xu, B. (2023). Experimental Study on Seismic Performance of CFRP-Strengthened Recycled Concrete Columns with Different Levels of Seismic Damage. *Buildings*,

13(6). https://doi.org/10.3390/buildings13061470

Tawil, S. El, & G. G. Deierlein. (1999). Strength and Ductility of Concrete Encased Composite Columns. *Journal Of Structural Engineering*.